3104–3110 *Nucleic Acids Research, 1998, Vol. 26, No. 13*

The orientation and dynamics of the C2′-OH and hydration of RNA and DNA·RNA hybrids

Jeffrey I. Gyi, Andrew N. Lane*, Graeme L. Conn[1,+] and Tom Brown[1]

Division of Molecular Structure, National Institute for Medical Research, The Ridgeway, Mill Hill, London NW7 1AA, UK and [1]Department of Chemistry, University of Southampton, Southampton SO17 1BJ, UK

Received April 6, 1998; Revised and Accepted May 18, 1998

ABSTRACT

The stereochemical and dynamic properties of the C2′ hydroxyl group in several DNA·RNA hybrids have been measured by NMR and compared with the homologous RNA duplex. The C2′-OH NMR signals of the RNA strands were identified, and numerous specific assignments were made. The rate constants for exchange of the hydroxyl protons with water were determined at 5°C, and were found to depend on both the position within a particular sequence and the nature of the duplex. On average, the exchange rate constants were slowest for the hybrids of composition rR·dY, and fastest for the RNA duplex, with an overall range of ~10–50/s. In the DNA·RNA hybrids, strong NOEs and ROEs were observed between the OH and the H1′ of the same sugar, unambiguously showing that the OH proton points toward the H1′ most of the time, and not toward the O3′ of the same sugar. Evidence for significant hydration in both grooves of the DNA·RNA hybrids and the DNA duplex was found in ROESY and NOESY experiments. On average, the minor groove of the DNA·RNA hybrids showed more kinetically significant hydration than the DNA, which can be attributed to the hydrophilic lining of hydroxyl groups in RNA.

INTRODUCTION

DNA·RNA hybrids are important biological intermediates involved in transcription, DNA synthesis and reverse transcription (1). They are also formed as translationally inactive products of antisense therapy, and are substrates for the enzyme RNase H. To understand the principles that determine the stability of hybrid duplexes, and thereby improve the design of antisense oligonucleotides, a knowledge of their conformational properties in solution is essential. The conformations of DNA·RNA hybrids are quite different from those of DNA and RNA duplexes at the nucleotide level. They also differ significantly in their global conformations, though they resemble the A-form of RNA more than the B-form of DNA (2–8). Furthermore, the thermodynamic stability of DNA·RNA hybrids, while always lower than that of the homologous RNA duplex, can be either more or less stable than the DNA duplex, depending on the base-composition of the strands (8–10). The thermodynamic stability and solution conformation of nucleic acids also depend on their interaction with ions and water (11–13). Nucleic acids are highly hydrated in aqueous solution (13,14). However, dehydration of DNA causes the conversion from the B-form into the A-form. In contrast, RNA in solution is invariably found in the A-conformation, regardless of the water activity (13). A large contribution to the stability of DNA and RNA duplexes is the favourable enthalpy associated with base-stacking (15), which is greater in the A-form than in the B-form. Hence, there is a strong inter-dependence of the chemical structure, conformation and interactions with water.

The hydroxyl group on the C2′ of ribose is likely to have a great influence on the hydration, conformation and thermodynamic stability of RNA compared with DNA. These groups, which line the shallow minor groove of RNA, are expected to be involved in extensive hydrogen bonding interactions with water (16–19). In contrast, the minor groove of A-DNA would be relatively hydrophobic, and therefore potentially destabilised by water. The interplay between conformation and hydration has also been shown in DNA, where the spine of hydration in the narrow minor groove of dAn·dTn sequences is significantly different from that observed in the minor grooves of mixed sequence DNA duplexes (13,14,20–24). However, much less information is available on the hydration of DNA·RNA hybrids. Recently, the hydroxyl protons were observed in a DNA·RNA hybrid by NMR spectroscopy (25). We report here the identification of C2′-OH groups in both RNA and DNA·RNA hybrid duplexes that we have been studying (8,26) and show that there are distinct differences in the behaviour of these protons and how they interact with water for the RNA and DNA·RNA hybrid duplexes.

MATERIALS AND METHODS

DNA and RNA oligonucleotides were synthesised and purified as previously described (8). We have examined the following duplex sequences:

d(GAAGAGAAGC)·d(GCTTCTCTTC) (dR10·dY10), d(GAAGAGAAGC)·r(GCUUCUCUUC) (dR10·rY10), d(GAAGAGAAGC)·r(GCTTCTCTTC) [dR10·rY(T)10], r(GAAGAGAAGC)·r(GCUUCUCUUC) (rR10·rY10), r(GAAGAGAAGC)·d(GCUUCUCUUC) [rR10·dY(U)10] and r(GAAGAGAAGC)·d(G^{p}C^{p}U^{p}U^{p}C^{p}U^{p}C^{p}U^{p}UC) (rR10·d^{p}Y10). In dR10·rY(T)10, each RNA uracil base is methylated at the 5-position, in rR10·dY(U)10, each deoxyribose thymidine base is demethylated at the 5-position, and in rR10·d^{p}Y10, ^{p}N is a pyrimidine base modified at the 5-position with the propyne group (-C≡C-CH_3).

*To whom correspondence should be addressed. Tel: +44 181 959 3666; Fax: +44 181 906 4477; Email: alane@nimr.mrc.ac.uk

+Present address: Department of Chemistry, Johns Hopkins University, Baltimore, MD 21218, USA

^{1}H NMR spectra were recorded at 500 or 600 MHz on a Varian Unity Plus or Unity spectrometer, respectively. Experiments were performed at 5°C in 90% H_2O:10% D_2O using the Watergate method (27) for suppressing the intense solvent peak. Spectra were recorded at a concentration of ~0.5 mM in 5 mm NMR tubes, or at ~0.15 mM in 8 mm tubes in the case of rR10·rY10 to eliminate aggregation of the solutes at low temperature. Phase-sensitive (28) NOESY and ROESY spectra were typically recorded with mixing times of 50 and 25 ms, respectively, as previously described (19,24). TOCSY spectra were recorded using MLEV-17 (29) with a mixing time of 40–46 ms and a spin-lock strength of 8 kHz. Assignments of the C2′-OH resonances of the RNA strands were achieved where possible using the observed NOEs between these protons and assigned H1′ and H2′ as previously described (19), and also the scalar coupling to the H2′ using TOCSY (29). The assignments of the modified duplexes dR10·rY(T)10, rR10·dY(U)10 and rR10·dPY10 were made using standard techniques as previously described (8) and will be published elsewhere.

Estimates of the exchange rate constant of the C2′-OH with water were made in several ways. First, the degree of saturation was measured by comparing relaxed 1D spectra with and without 3s presaturation of the water resonance. This gives the steady-state magnetisation transfer from water to the C2′-OH, which is determined by the dissociation rate constant and the intrinsic spin-lattice relaxation rate constant of the OH, according to equation **1**:

$$M/M^0 = \rho/(\rho+k) \qquad \mathbf{1}$$

where M is the steady state magnetisation, M^0 is the magnetisation in the absence of presaturation, k is the dissociation rate constant and ρ is the intrinsic spin-lattice relaxation rate constant. To estimate ρ, we calculated a range based on the internuclear distances between the OH and its neighbours using models of the structures (26), according to:

$$\rho = \Sigma(1/r^6)[J(0) + 3J(\omega) + 6J(2\omega)] \qquad \mathbf{2}$$

where r is the internuclear distance, J(nω) is the spectral density function and ω is the Larmor frequency.

The correlation time was calculated for H_2O from the values measured in D_2O at 30°C (8) and using the fact that the viscosity of water is ~24% lower than that of D_2O, and tabulated values of the viscosity of water at different temperatures (30).

A second estimate of k was obtained from measurements of the linewidth of the OH peaks from OH-H1′ cross-peaks in NOESY spectra. The linewidth depends on numerous factors as follows:

$$L = L_0 + L(\Delta B) + \Sigma J + k/\pi \qquad \mathbf{3}$$

where L_0 is the intrinsic linewidth, L(ΔB) is the contribution from magnetic field heterogeneity and limited digital resolution and ΣJ is the contribution from unresolved scalar coupling (e.g. to H2′). The intrinsic linewidth was estimated in a manner similar to that described for the spin-lattice relaxation rate constant, L(ΔB) was estimated as the measured linewidth of DSS in the same spectrum, and ΣJ was assumed to be at least 4 Hz on the basis of the observed TOCSY cross-peaks. This calculation should provide an upper limit to the rate constant for exchange with water, as other contributions are not considered, such as fast intermediate exchange among different rotamer states of the hydroxyl group.

A third estimate was obtained by integrating the cross-peaks between OH and water in the NOESY spectra, and normalising them to the sum of the diagonal and cross-peaks volumes. For short mixing times, the exchange cross-peaks depend on mixing time, t_m, approximately as:

$$M(X)/[M(X)+M(D)] = -k\cdot t_m \qquad \mathbf{4}$$

A fourth estimate was obtained from 1D EXSY experiments (31).

Because of the necessary approximations involved in these calculations, the absolute values of k are unlikely to be very accurate. However, consistency between the methods indicates that the exchange rate constants are determined within reasonable limits.

Simulations of magnetisation transfer between water, OH and H1′ were made under a variety of assumptions, namely the exchange rate constant, the spin-lattice relaxation rate constants, and the cross-relaxation rate constant between OH and H1′ (i.e. the effects of geometry). For a three-spin system of this kind, analytical expressions can be obtained for the time course of magnetisation transfer, and which then provide a useful guide to the interpretation of the observed results. Additional calculations were made from complete structures using the program NUCFIT (32).

RESULTS

Assignments of C2′-OH

Figure 1 shows 1D spectra of rR10·rY10, rR10·dPY10, rR10·dY(U)10, dR10·rY(T)10, dR10·rY10 and dR10·dY10 recorded in H_2O, at 5°C. The assignments of the non-exchangeable protons, and the amino protons of Cyt have been previously described (8). However, there are additional peaks between 6.5 and 7.0 p.p.m. that are not present in D_2O solutions, and cannot be attributed to amino protons. Using a combination of TOCSY, ROESY and NOESY spectra with short mixing times (Fig. 2) we have confirmed that these resonances arise from the ribose C2′-OH (19). The TOCSY peaks confirm the significant coupling between C2′-OH and the C2′-H. In the case of the hybrid duplexes dR10·rY(T)10 and rR10·dPY10, there is sufficient dispersion in the C2′-OH region that several individual OH resonances can be assigned, as shown in Figure 2 and Table 1. This gives much more detail of the sugar hydroxyl of RNA in solution than has previously been observed.

Exchange rate constants

The exchange cross peaks between the C2′-OH and water in the ROESY spectra demonstrate that the exchange process is relatively slow on the chemical shift time scale. Furthermore, it must be sufficiently slow so as not to bleach out ROEs and NOEs between the C2′-OH and H1′ or H2′. Thus, the exchange is much slower than is found for simple sugars. The exchange rate constant for different C2′-OH groups in the various duplexes was estimated as described in the methods, and we find a range from ~10 to 50/s, with the largest rate constants found for the RNA duplex, and the lowest for the rR10·dPY10 duplex (Table 1). These values are an order of magnitude larger than found for the UUCG tetraloop (33), but comparable with the values estimated at 5°C for a DNA·RNA hybrid (25). The exchange rate constants are considerably lower than for a free nucleotide; the C2′-OH was not detected in rUMP under similar solution conditions (A.N.Lane and J.I.Gyi, unpublished results). Furthermore, the 3′-terminal nucleotide of dR10·rY(T)10 showed no hydroxyl

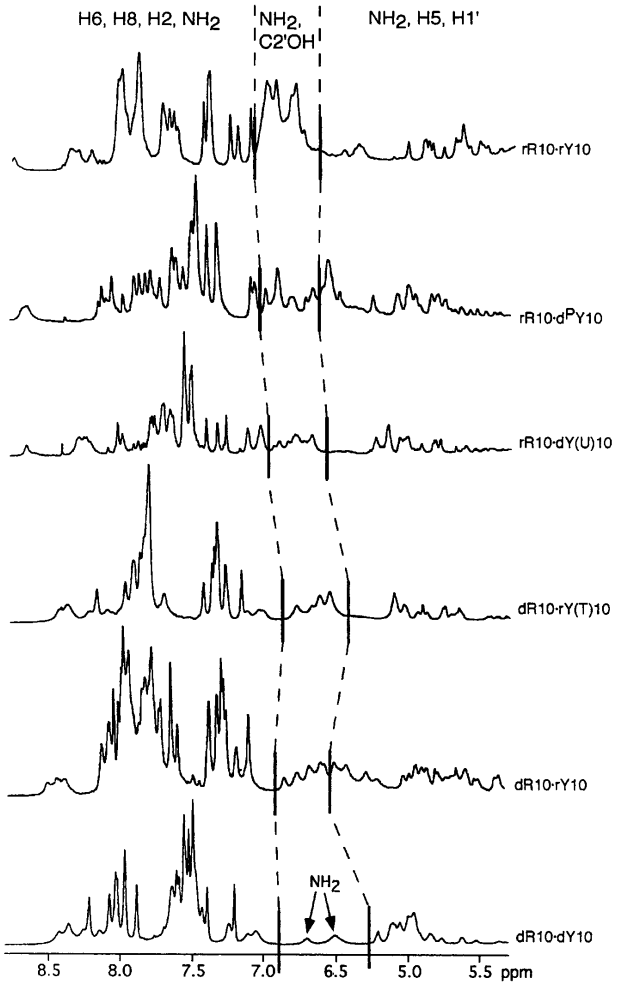

Figure 1. 1D ^{1}H NMR spectra of rR10·rY10, rR10·dPY10, rR10·dY(U)10, dR10·rY(T)10, dR10·rY10 and dR10·dY10. NMR spectra were recorded at 5°C in H_2O as described in Materials and Methods.

cross-peaks, indicating much faster exchange. This C2′-OH cannot hydrogen bond to a 3′ residue and must be completely exposed to solvent. Hence, because the minor groove is exposed to solvent, it is probable that the observed relatively low exchange rate constants are due to H-bonding between the C2′-OH and unknown acceptor groups. The likely presence of hydrogen bonding interactions would be expected to result in restricted rotation about the C2′-O2′ bond, and to a preference for one of the three rotamer states (see below). The linewidths, measured from cross-sections in the NOESY spectra, reflect the relative exchange rate constants (compare with equation 3). This provides only an upper estimate of k because of unknown contributions from unresolved J-coupling between the C2′-OH and C2′H, which can vary from ~0 to 12 Hz, and the intrinsic linewidth, which we estimate to be of the order of 2–3 Hz. An additional contribution to the linewidth could also arise from exchange among rotamers on the chemical shift timescale. Because the saturation transfer experiments show that most of the linewidth arises from exchange with water (Table 1), this contribution should be small in comparison with the others, but could contribute relatively more to the RNA (broad hydroxyl protons) than to the hybrids. We note also that the apparent linewidths or exchange rate constants (Table 1) do not correlate with thermodynamic stability (8; G.L.Conn, unpublished data).

Table 1. ^{1}H NMR assignments of C2′-OH resonances and exchange rate constants

Duplex	δ(C2′-OH)/p.p.m.	assignment	L/Hz	k_x(L)/s	k_x(RY)/s
rR10·rY10	6.77	nd			
	6.82	C15/17	26	<66	24 ± 5
	6.85	U14	26	<66	24 ± 5
	6.96	G4,6	26	<66	24 ± 5
dR10·rY10	6.86	U19	9.3	14	12
	6.68	U14	10	16	12
[a]dR10·rY(T)10	6.64	U14	19	44	20
	6.78	U19	23	56	20
	6.68	C17/U18	15	31	21
	6.56,6.62	nd	18	41	nd
rR10·dY(U)10	6.71	A2,A3,A7	16	35	nd
	6.80	A8	15	16	nd
	6.81–6.84	G1,G4,G6	13	25	38
	6.88	G9	14	28	38
[b]rR10·dPY10	6.81	A2,A5	12	22	24
	6.70	A3	8	9.5	19
	6.93	G4	16	35	nd
	6.96	G6	9	13	nd
	6.69	A7	6	7	19
	6.74	A8	15	35	20

Assignments were made at 5°C from TOCSY, NOESY and ROESY spectra as described in the Materials and Methods. L is the linewidth at half peak height corrected for magnetic inhomogeneity. k_x(L) is the exchange rate constant estimated from the linewidth L assuming unresolved scalar couplings and intrinsic dipolar contributions of 5 Hz, and k_x(RY) is the value estimated from the cross-peak intensity in a short mixing time ROESY or NOESY experiment.
[a]saturation transfer k≈30/s.
[b]saturation transfer k≈15/s

Orientation of the C2′-OH

Although the ROESY spectrum indicates that the C2′-hydroxyl protons are in slow exchange with the solvent, in the DNA·RNA hybrids they show intense NOEs to both the C2′-H and H1′. This was confirmed by the observation of scalar cross-peaks in a TOCSY recorded with a mixing time of 40 ms, in which clear cross-peaks were obtained between the exchangeable protons in the 6.5–7 p.p.m. range, and the C2′-H, but not H1′ (Fig. 2). Also, there were only weak NOEs between the H1′ and the water resonance, which were exclusively those of the RNA strands. This indicates that either the H1′ of the DNA strands are not close to water protons, or the water residence time is extremely short (i.e. the H1′ are not solvated in either a thermodynamic or a kinetic sense). The same was true for the pure DNA duplex. The ready observation of the C2′-OH, and its relatively intense NOEs to both the H2′ and H1′ implies that the exchange rate of the hydroxyl proton with water is quite low under these conditions (see above). The large C2′-OH–H1′ NOE (comparable with that

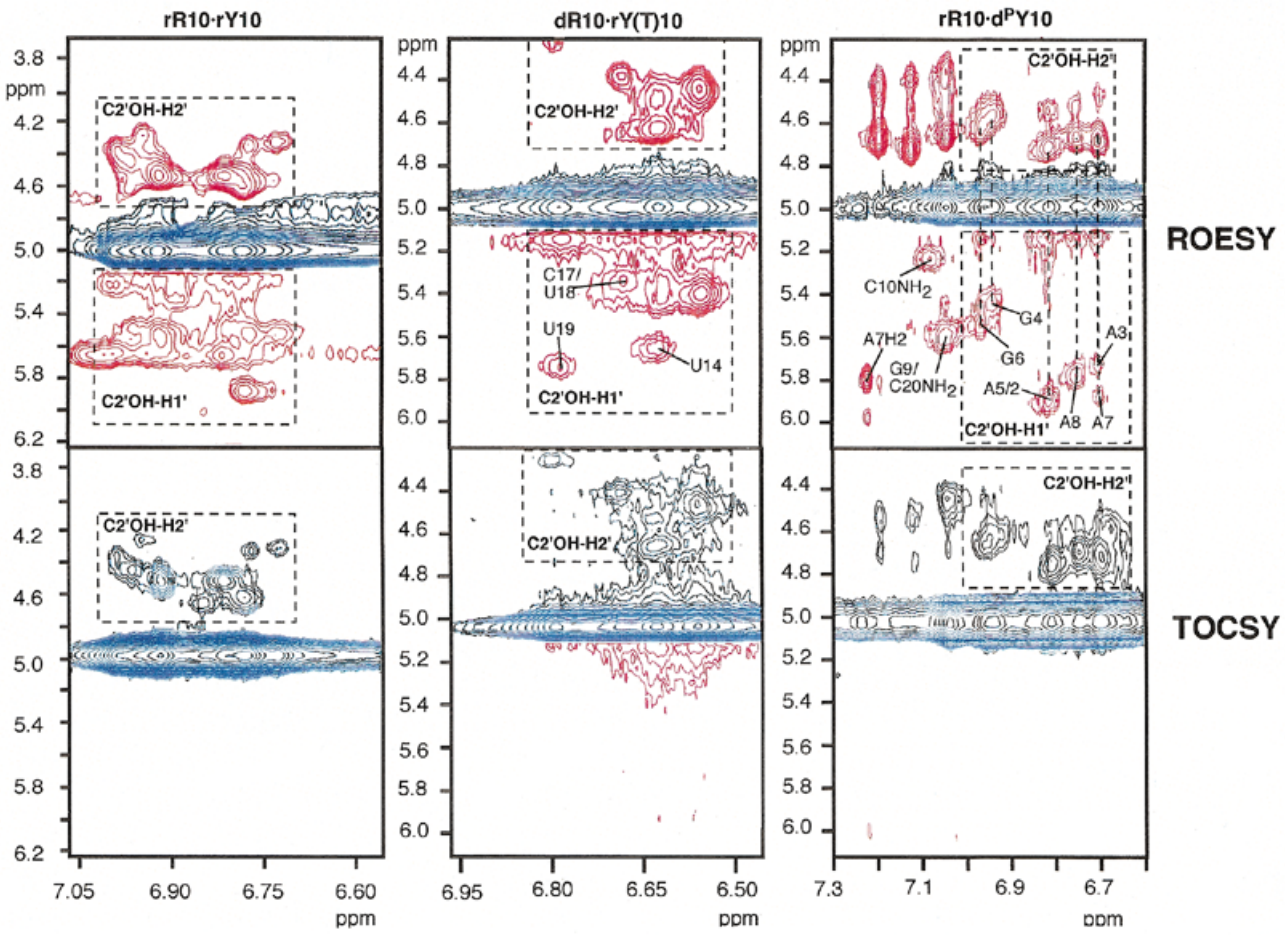

Figure 2. TOCSY and ROESY spectra of the RNA and DNA·RNA hybrids: assignment of C2′-OH. The spectra were recorded at 5°C and 600 MHz with mixing times of 46 (TOCSY) and 25 ms (ROESY). Positive peaks are in blue, negative peaks are in red. Assignments of the C2′-OH resonances of the RNA strands were achieved where possible using the observed NOEs between these protons and assigned H1′ and H2′, and also the scalar coupling to the H2′ using TOCSY. In each case, the top panel shows the ROESY spectrum, and the bottom panel the analogous region of the TOCSY spectrum. From left to right: rR10·rY10 [ROESY, τ_m = 25 ms, spectral width (F1/F2) = 10 000 Hz, acquisition times t_1 = 0.04 s, t_2 = 0.5 s; TOCSY, τ_m = 46 ms, spectral width (F1/F2) = 10 000 Hz, acquisition times t_1 = 0.04 s, t_2 = 0.5 s], dR10·rY(T)10 [ROESY, τ_m = 25 ms, spectral width (F1/F2) = 13 000 Hz, acquisition times t_1 = 0.02 s, t_2 = 0.5 s; TOCSY, τ_m = 46 ms, spectral width (F1,F2) = 12 000 Hz, acquisition times t_1 = 0.03 s, t_2 = 0.5 s], rR10·dPY10 [ROESY, τ_m = 25 ms, spectral width (F1,F2) = 13 000 Hz, acquisition times t_1 = 0.02s, t_2 = 0.5 s; TOCSY, τ_m = 46 ms, spectral width (F1,F2) = 13 000 Hz, acquisition times t_1 = 0.02 s, t_2 = 0.5 s].

of H1′-H2′ in the RNA strands or H1′-H2′ resonances in the DNA strands) for the non-terminal residues indicates that these two protons are close together for at least some of the time, which requires that the hydroxyl proton points away from the O3′ of the same residue.

Table 2. NOEs and ROEs observed in the duplexes

	Cross-peak intensities				
Duplex	C2′-OH-H2′	C2′-OH-H1′	H1′-H_2O	AH2-H_2O	H6/H8-H_2O
rR10·rY10	m/s	m	0/w	w	w
rR10·dY(U)10	s	m	0/w	0	0/w
rR10·dPY10	s	s	w/m	m	m
dR10·rY(T)10	s	s	w/m	m	m
dR10·rY10	s	s	w	m	m
dR10·dY10	–	–	0/w	m	m

Cross-peak strengths are denoted as s (strong), m (medium), w (weak) or 0 (not visible) according to relative areas in cross-sections at the water frequency (compare with Fig. 4).

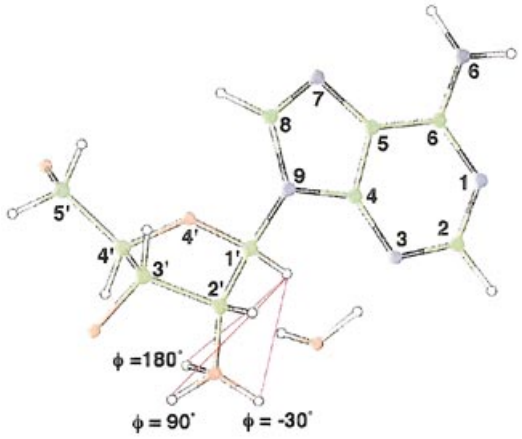

Figure 3. Model adenosine nucleotide showing a superimposition of the three favoured rotamers of C2′-OH. The torsion angle labelled ϕ refers to that formed between O2′H and H2′. The rotation is about the bond C′-O2′.

The pattern of NOEs in the DNA duplex is quite different from that observed in the hybrid duplexes (Table 2). The DNA duplex has no C2′-OH, so that NOEs involving these protons are not present. This is further supporting evidence that the NOEs observed in the RNA-containing duplexes involve the hydroxyl protons. In the RNA decamer, NOEs were observed between the C2′-OH and the H2′ (and a strong exchange cross-peak with water) and between the C2′-OH and the H1′. The pattern of NOEs is different than previously observed in an RNA oligomer having a mixed sequence (19), and distinct thermodynamic and conformational properties (34).

Molecular models of the RNA duplexes and the DNA·RNA hybrids show that there are three stable rotamers for rotation about the C2′-O2′ bond (Fig. 3). In these states, the C2′-OH can hydrogen bond to O3′ of the 3′-phosphate [ϕ = 90 (*trans*), when the C2′-OH-H1′ distance is large, ~3.5 Å, and $^3J_{H2'\text{-}C2'\text{-}OH}$ < 4 Hz], to the O4′ of either the neighbouring 3′-ribose or in the same sugar (ϕ = 180°, when the C2′-OH-H1′ distance is short, <2.5 Å, $^3J_{H2'\text{-}C2'\text{-}OH}$ = 10–12 Hz), or toward the attached base (ϕ = 0 to –30°, when the C2′-OH-H1′ distance <2.5Å, and $^3J_{H2'\text{-}C2'\text{-}OH}$ = 4–7 Hz) (Fig. 3). These orientations have been proposed based on high resolution X-ray structures of RNA (16–18) and long molecular dynamics simulations (35,36). In mixed sequence RNA the favoured position for the C2′-OH is toward the O3′ (i.e. ϕ = 90°) and the sequential H-bond to O4′(i + 1) is not stereochemically reasonable (16,35).

The presence of the C2′-OH-H2′ TOCSY cross-peaks, and the strong NOE or ROE between C2′-OH and H1′ for all of the DNA·RNA hybrids and the RNA duplex (Fig. 2, Table 2) is not consistent with the dominant rotamer ϕ = 90°. In rR10·dPY10, the linewidths of the C2′-OH of A3, G6 and A7 are in the range 6–9 Hz (Table 1). Given a natural linewidth of 2–3 Hz, this places an upper limit to $^3J_{H2'\text{-}C2'\text{-}OH}$ of 4–7 Hz. A lower limit of >3 Hz is implied by the intense TOCSY peak with a 40 ms spin-lock time. Hence, for these hydroxyls, the preferred orientation must be ϕ = 0 to –30°. The interaction of the C2′-OH with water may suggest that the bridging interaction to the attached base is the preferred orientation in the hybrids. In the other duplexes, the same pattern of NOESY and TOCSY intensities is observed, but it is possible that the orientation with ϕ = 180° is also populated. The RNA duplex also shows that in this case, the O3′ orientation (ϕ = 90°) is not the dominant conformer. However, the exchange rate constant is, on average, higher in the RNA duplex than in the hybrids (Table 2), suggesting that it is hydrogen bonded for less time. This may be as a result of conformational differences between the two classes of molecules (8,26), and the preferred orientations may be composition- or sequence-dependent. Presumably, the difference in the local minor groove geometry between the RNA duplex and the hybrids (2–8) is the cause of the difference in H-bond patterns.

Hydration

In addition to the obvious chemical and conformational differences between DNA and RNA duplexes, the pattern of hydration of non-exchangeable protons is also different. We have therefore examined some aspects of hydration of these duplexes using NMR. Figure 4 shows cross-sections through the water frequency in both ROESY and NOESY spectra recorded under identical conditions except for the mixing times which were 25 ms for the ROESY and 50 ms for the NOESY experiments.

Water-base proton NOEs and ROEs show that the major groove is accessible to solvent. The methyl groups of thymine, where present, showed positive NOEs, indicating a short (<0.3 ns) correlation time. This probably reflects the rapid reorientation of the methyl group. The methyl of the propyne group in rR10·dPY10 also showed positive NOEs and ROEs at the water frequency. Thus, the major groove in both the DNA·RNA hybrids and the DNA duplex is accessible to water. Figure 4 also shows that the purine H8 and pyrimidine H6 protons of non-terminal bases showed negative NOEs (and positive ROEs), indicating effective correlation time longer than ~0.3 ns (24). In the two hybrids dR10·rY(T)10 and rR10·dPY10, although the H8/H6 showed interaction with water, overlap with exchangeable amino protons precluded quantitation. Also, as the water relaxation may be slower in ROESY than in NOESY because of radiation damping in the latter, the ROESY intensity may be greater than in the NOESY. In contrast, the major groove protons of the RNA duplex showed only weak interactions with water (Fig. 4, Table 2), suggesting either restricted access in the deep, narrow major groove of RNA, or very short residence times for major groove water.

In both the DNA duplex and the DNA·RNA hybrids, significant negative NOEs and positive ROEs were found between water and the Ade H2 in the minor groove (Fig. 4). The intense cross-peaks observed for the H2 indicate ready access of the minor groove to water, and with a residence time >0.3 ns (24). In addition, significant NOEs and ROEs were also observed to the H1′ exclusively in the RNA strands of these hybrids, and weaker cross-peaks to H1′ in the RNA duplex (Fig. 4).

Water-H1′ NOEs are complicated by the exchange between the C2′-OH and water. Because a strong ROE was observed between the C2′-OH and the H1′ (Fig. 2), it is clear that the hydroxyl proton is close (<2.5 Å) to the H1′, so that magnetisation can be relayed by exchange with water through the hydroxyl proton. Figure 5 shows representative ROESY time courses (normalised to that of the Cyt H5-H6 cross-peak) for magnetisation transfer by this pathway for different values of the exchange rate constant (5–50/s) and the cross-relaxation rate constant. As expected, the degree of transfer is insignificant for a cross-relaxation rate constant of 0.4/s (corresponding to the O3′ orientation) for any value of the exchange rate constant up to at least 50/s. Transfer is efficient only for the other two rotameric positions, where σ≈2.4/s. This suggests

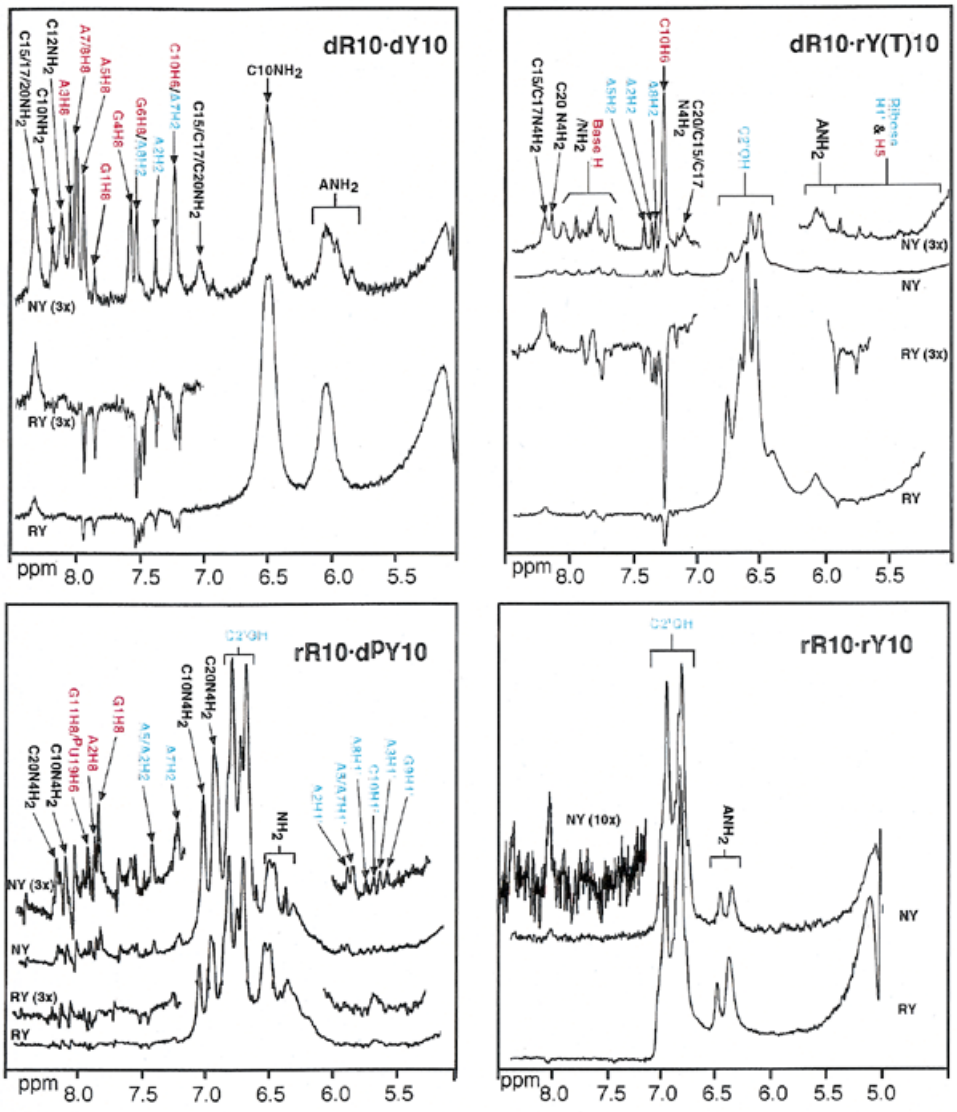

Figure 4. Cross-sections through NOESY and ROESY spectra. NOESY (NY) and ROESY (RY) spectra were recorded at 5°C, 600 MHz with mixing times of 50 and 25 ms respectively. The cross-sections are taken at the water frequency, along the F2 dimension. Cross peaks show interaction of solute protons with water via dipolar interactions or chemical exchange. Protons in red are in the major groove, those in blue are in the minor groove, and exchangeable protons, with the exception of C2′OH, are shown in black.

that in the hybrids at least, the observed water-H1′ NOEs and ROEs arise primarily via the exchange-mediated pathway, so it is impossible to determine whether there is any direct interaction between water and H1′. Nevertheless, the exchange of the C2′-OH indicates extensive solvation of the minor groove of both the hybrids and the RNA duplex, and in the hybrids especially, the interaction of water with Ade C2H indicates that the groove as a whole has extensive and relatively long-lived contact with water. Molecular dynamics simulations indicate that long lived waters in the minor groove of RNA are associated with bridges between oxygen atoms of neighbouring phosphates in the backbone, or as bridges between the C2′-OH and the base (35,36). It is notable that the residence time of water that makes a single H-bond to the solute is very short.

The DNA·RNA hybrids show interactions with water that have characteristics in common with both the DNA duplex and the RNA duplex. In the major groove, the accessibility to water in the hybrids is more similar to the DNA duplex than to the RNA duplex. The minor groove also shows evidence of relatively stable hydration around the Ade C2H, comparable with that in the DNA duplex. The C2′-OH has a preferred orientation, and interacts directly with water. In the RNA duplex, access to water or its kinetic stability in the major groove is less than in the DNA duplex or the DNA·RNA hybrids. However, the C2′-OH also has a preferred orientation (though not necessarily as stable as that in the hybrids), and interacts directly with the water.

ACKNOWLEDGEMENTS

This work was supported by the MRC and Oswel Research Products Ltd. GLC gratefully acknowledges a Royal Society of Edinburgh Caledonian Research Fellowship.

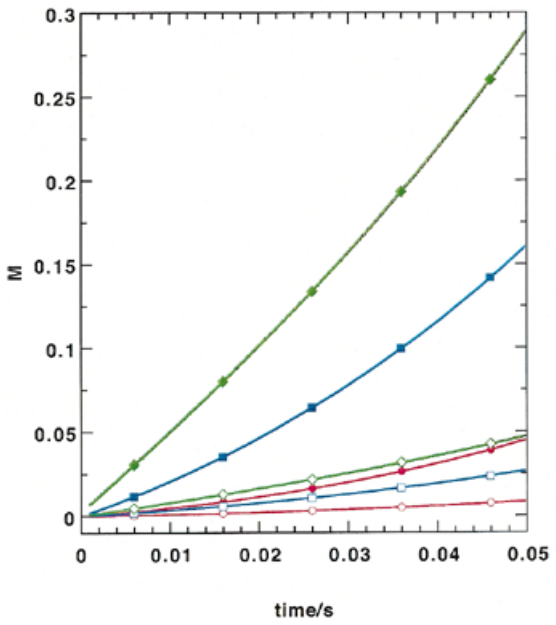

Figure 5. Simulated ROE time courses in the absence and presence of exchange with solvent. Time courses were calculated analytically for a three-spin system comprising water, C2′-OH and H1′ assuming exponential relaxation of the water resonance. The curves shown were calculated for different values of the exchange rate constant (k) and the cross-relaxation constant for C2′-OH-H1′ (σ). ρw (water), ρ1′ (H1′) and ρ_{OH} (C2′-OH) were set to 1, 7 and 12/s based on calculations as described in Materials and Methods. The magnetisation has been normalised to that of the cytosine H5-H6 cross peak calculated for standard A-RNA. ○, σ = 0.4/s and k = 5/s; ●, σ = 2.4/s and k = 5/s; □, σ = 0.4/s and k = 25/s; ■, σ = 2.4/s and k = 25/s; ◇, σ = 0.4/s and k = 50/s; ◆, σ = 2.4/s and k = 50/s.

REFERENCES

1 Voet, D. and Voet, J.G. (1995) *Biochemistry* 2nd Edition, John Wiley and Sons, New York.
2 Lane, A.N., Ebel, S. and Brown, T. (1993) *Eur. J. Biochem*. **215**, 297–306.
3 Salazar, M., Champoux, J.J. and Reid, B.R. (1993) *Biochemistry* **32**, 739–744.
4 Salazar, M., Fedoroff, O.Y., Miller, J.M., Ribeiro, N.S. and Reid, B.R. (1993) *Biochemistry* **32**, 4207–4215.
5 Fedoroff, O.Y., Salazar, M. and Reid, B.R. (1993) *J. Mol. Biol.* **233**, 509–523.
6 Gonzalez, C., Stec, W., Kobylanska, A., Hogrefe, R.I., Reynolds, M. and James, T.L. (1994) *Biochemistry* **33**, 11062–11072.
7 Gonzalez, C., Stec, W., Reynolds, M. and James, T.L. (1995) *Biochemistry* **34**, 4969–4982.
8 Gyi, J.I., Conn, G.L., Brown, T. and Lane, A.N. (1996) *Biochemistry* **35**, 12538–12548.
9 Lesnik, E.A. and Freier, S.M. (1995) *Biochemistry* **34**, 10807–10815.
10 Ratmeyer, L., Vinayak, R., Zhong, Y.Y., Zon, G. and Wilson, W.D. (1994) *Biochemistry* **33**, 5298–5304.
11 Manning, G.S. (1978) *Q. Rev. Biophys*. **11**, 179–246.
12 Record, M.T., Anderson, C.F. and Lohman, T.M. (1978) Q*. Rev. Biophys*. **11**, 103–178.
13 Saenger, W. (1984) *Principles of Nucleic Acid Structure*. Springer-Verlag, New York, chapter 7.
14 Chalikian, T.V., Sarvazyan, A.P., Plum, G.E. and Breslauer, K.J. (1994) *Biochemistry* **33**, 2394–2401.
15 Searle, M.S. and Williams, D.H. (1993) *Nucleic Acids. Res*. **21**, 2051–2056.
16 Egli, M., Portmann, S. and Usman, N. (1996) *Biochemistry* **35**, 8489–8484.
17 Wahl, M.C., Ban, C., Sekharudu, C., Ramakrishnan, B. and Sundaralingam, M. (1996) *Acta Cryst*. **D52**, 655–667.
18 Leonard, G.A., McAuley-Hecht, K.E., Ebel, S., Lough, D.M., Brown, T. and Hunter, W.N. (1994) *Structure* **2**, 483–494.
19 Conte, M.R., Conn, G.L., Brown, T. and Lane, A.N. (1996) *Nucleic Acids Res*. **24**, 3693–3699.
20 Privé, G. G., Heinemann, U., Chandrasegaran, S., Kan, L.-S., Kopka, M.L. and Dickerson, R.E. (1987) *Science* **238**, 498–504.
21 Liepinsh, E., Otting, G. and Wüthrich, K. (1992) *Nucleic Acids Res*. **20**, 6549–6553.
22 Liepinsh, E., Leupin, W. and Otting, G. (1994) *Nucleic Acids Res*. **22**, 2249–2254.
23 Fawthrop, S.A., Yang, J.-C. and Fisher, J. (1993) *Nucleic Acids Res*. **21**, 4860–4866.
24 Lane, A.N., Jenkins, T.C. and Frenkiel, T.A. (1997) *Biochim. Biophys. Acta* **1350**, 205–220.
25 Federoff, O.Y., Ge, Y. and Reid, B.R. (1997) *J. Mol. Biol*. **269**, 225–239.
26 Gyi, J.I., Conn, G.L., Brown, T. and Lane, A.N. (1998) *Biochemistry* **37**, 73–80.
27 Piotto, M., Saudek, V. and Sklenar, V. (1992) *J. Biomol. Str*. **2**, 661–665.
28 States, D.J., Haberkorn, R.A. and Ruben, D.J. (1982) *J. Magn. Reson*. **48**, 286–292.
29 Bax, A. and Davies, D.G. (1985) *J. Magn. Reson*. **65**, 355–360.
30 Millero, F.J., Dexter, R. and Hoff, E. (1971) *J. Chem. Eng. Data* **16**, 85–87.
31 Bulliman, B.T., Kuchel, P.W. and Chapman, B.E. (1989) *J. Magn. Reson*. **82**, 131–138.
32 Lane, A.N. (1990) *Biochim. Biophys. Acta* **1049**, 189–204.
33 Lynch, S.R., Pelton, J.G. and Tinoco, I.,Jr (1996) *Magn. Reson. Chem*. **34**, S11–S17.
34 Conte, M.R., Conn, G.L., Brown, T. and Lane, A.N. (1997) *Nucleic Acids Res*. **25**, 2627–2634.
35 Auffinger, P. and Westof, E. (1997) *J. Mol. Biol*. **269**, 326–341.
36 Auffinger, P. and Westof, E. (1997) *J. Mol. Biol*. **274**, 54–63.